C. R. Mecanique 344 (2016) 60–67

Contents lists available at ScienceDirect

Comptes Rendus Mecanique

www.sciencedirect.com

Fluctuating pressure measurements in a turbulent separation bubble ☆

Mesures de pression instationnaire dans un bulbe de décollement turbulent

Julian Trünkle, Abdelouahab Mohammed-Taifour, Julien Weiss *

Laboratoire TFT, École de technologie supérieure, Montréal, QC H3C 1K3, Canada

ARTICLE INFO

Article history:
Received 9 April 2015
Accepted 11 September 2015
Available online 11 November 2015

Keywords:
Turbulence
Separated flows
Unsteady pressure

Mots-clés :
Turbulence
Écoulements décollés
Pression instationnaire

ABSTRACT

Fluctuating pressure measurements are performed on the test surface above a pressure-induced, turbulent separation bubble. The Reynolds number of the incoming turbulent boundary layer is $Re_\theta \simeq 5000$. The results confirm the presence of a low-frequency breathing mode, caused by the contraction and expansion of the bubble, and a medium-frequency shedding mode, caused by the roll-up and shedding of spanwise vortices in the shear layer bordering the recirculating region. The signatures of both modes are shown to be consistent throughout the span of the test section. In addition, another fluctuating mode is observed and related to the presence of slowly rotating vortices close to the test-section sidewalls.

RÉSUMÉ

Des mesures de pression instationnaire sont effectuées dans une zone de décollement turbulente générée sur une surface plane par une combinaison de gradients de pression adverse et favorable. Le nombre de Reynolds de la couche limite amont est de $Re_\theta \simeq 5000$. Les résultats confirment la présence d'un mode de « respiration » basse fréquence causé par la contraction et l'expansion de la zone décollée, ainsi que d'un mode convectif causé par l'enroulement et le lâcher de structures tourbillonaires au sein de la couche de mélange. La signature des deux modes est observée sur toute l'envergure de la surface d'essai. De plus, un troisième mode fluctuant est observé à proximité des parois latérales, relié à la présence de tourbillons trombes.

☆ A related version of this article was first presented at the 50th 3AF International Conference on Applied Aerodynamics (Toulouse, France) on March 30th, 2015.

* Corresponding author.
E-mail address: julien.weiss@etsmtl.ca (J. Weiss).

http://dx.doi.org/10.1016/j.crme.2015.09.003
1631-0721/

1. Introduction

Separation and reattachment of turbulent boundary layers (turbulent separation bubbles) are known to be associated with low-frequency pressure and velocity fluctuations. This can have practical implications in a wide range of aerodynamic systems, where the fluctuations may be a source of vibrations, noise, or unsteady mechanical and thermal loads.

At subsonic speeds, most of the research performed so far concerns the case of *fixed-separation* flows, where the separation line is fixed by a geometric singularity (*e.g.* backward-facing step, blunt plate, or fence). Numerous experimental and numerical investigations have shown that these flows are characterized by two distinct unsteady modes [1–3]: a "flapping mode", which consists in a low-frequency up-and-down motion of the shear layer bounding the recirculating region, and a "shedding mode", which occurs because of the roll-up of vortical structures within the shear layer and their shedding downstream of the separated flow. When scaled with the separation-bubble length L_b and the velocity U_∞ of the incoming flow, the flapping mode has a normalized frequency $St_f \simeq 0.08$–0.2 and the shedding mode $St_s \simeq 0.5$–1.0 [4].

At supersonic speeds, turbulent separation bubbles occur in *shock wave/turbulent boundary-layer interactions* when the strength of the compression is strong enough to cause a separation of the incoming boundary layer. Experiments and numerical simulations in different flow configurations (*e.g.*, compression ramps, impinging shocks, or blunt cylinders) have shown that this type of flow is characterized by a large-scale, low-frequency oscillation of the separation shock and the bubble [5]. The Strouhal number typically associated with this unsteadiness is $St_{sbli} \simeq 0.03$, which is lower than that of the flapping motion of fixed-separation flows [6]. Evidence of a shedding mode at a Strouhal number close to 0.5 has also been provided in the case of an impinging-shock experiment at Mach 2.3 [7].

Recently, Weiss et al. [8] investigated the wall-pressure fluctuations within an incompressible, massively separated, turbulent separation bubble generated on a flat plate by a combination of adverse and favorable pressure gradients. They showed the presence of the shedding mode at a Strouhal number $St \simeq 0.35$ and interpreted its lower value compared to fixed-separation flows by a larger vorticity thickness of the shear layer. Weiss et al. [8] also demonstrated the existence of a "breathing" mode, which is associated with a low-frequency contraction/expansion of the separation bubble, and which generates pressure fluctuations upstream of detachment and downstream of reattachment at a Strouhal number $St \simeq 0.01$, that is, at a normalized frequency about 10 times lower than the flapping frequency of fixed-separation flows. This breathing mode was also shown in [8] to be strikingly similar to the low-frequency unsteadiness observed in shock-induced separated flows, thus leading to the hypothesis that the latter unsteadiness might not necessarily be a compressible phenomenon.

The measurements of Weiss et al. [8] were all performed on the centerline of their test section, although the wall streamlines were shown to be highly three-dimensional [9]. Thus, there remains a possibility that their results might be influenced by the near-wall, 3D structure of the flow. The purpose of the present paper is to provide further results of fluctuating wall-pressure measurements in the same flow configuration as Weiss et al. [8], with a particular emphasis on spanwise variations of the fluctuating wall pressure.

2. Experimental setup

Experiments were performed in the TFT Boundary-Layer Wind Tunnel, which is of a classical, blow-down type [9]. The test section has a total length of 3 m and a constant width of 0.6 m throughout its length. At its entrance ($x = 0$), the test-section height is 0.15 m. In the first half of the test section, the boundary layer developing on the test surface is not subjected to any pressure gradient. This is achieved by a slight divergence of the test-section floor, which maintains a zero-pressure-gradient (ZPG) condition up to the midpoint of the test section ($x = 1.5$ m). The boundary layer is then subjected to a strong adverse pressure gradient followed soon thereafter by a favorable pressure gradient. This creates a massively separated bubble on the test surface.

Fig. 1 shows a sketch of the test section in the region of the pressure-gradient zone. The boundary-layer bleed ensures that the separation bubble always occur on the flat test surface. The Reynolds number, based on momentum thickness, is $Re_\theta \simeq 5000$ at a streamwise position of $x = 1.1$ m and for a reference velocity of $U_{ref} = 25$ m/s. It was verified by Mohammed-Taifour et al. [9] that the incoming boundary layer has the characteristics of a "canonical" ZPG boundary layer. For reference, at $x = 1.1$ m the boundary-layer thickness is about 3 cm, and across the span of the test section the integral thicknesses are constant within 5% and the friction coefficient within 7%. The turbulence level in the potential-flow region is about 0.05%, but low-frequency ($f \leq 30$ Hz) fluctuations in mass flow originating in the centrifugal blower increase the total longitudinal velocity fluctuations up to about 0.3% [9].

Fig. 2 shows an oil-film visualization of the separated flow region at $U_{ref} = 25$ m/s. As discussed in [9], the topology of the limiting streamlines is very similar to the case of fixed separation flows. In particular, two slowly rotating vortices can be observed at the outside edges of the mean detachment line, near the side walls. On the test section centerline, the length of the separated-flow region was measured to be $L_b = 0.42$ m using a thermal-tuft probe [10]. Based on these measurements, a non-dimensional length x^* is defined so that $x^* = 0$ at the position of mean detachment and $x^* = 1$ at the position of mean reattachment [8]. Similarly, a normalized spanwise position z^* is defined so that $z^* = \pm 1$ correspond to the test-section side walls.

Measurements of the wall static-pressure fluctuations were performed at 20 streamwise positions ranging from $x^* = -1.67$ to $x^* = 2.86$ and at 7 spanwise positions ($z^* = 0$, $z^* = \pm 1/3$, $z^* = \pm 1/2$, and $z^* = \pm 2/3$). The fluctuating static pressure was measured with a Meggitt 8507C-1 piezoresistive pressure transducer that was either mounted flush to the

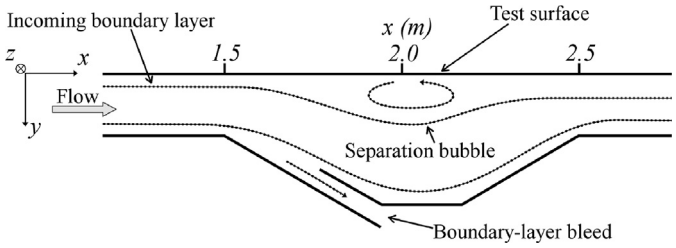

Fig. 1. Test section of the TFT Boundary-Layer Wind Tunnel [8].

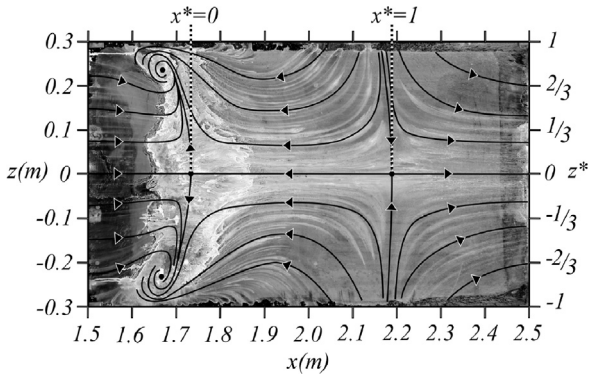

Fig. 2. Oil-film visualization of the separated-flow region, $U_{\text{ref}} = 25$ m/s.

test surface using a specially designed plug, or connected to a static-pressure tap with a flexible tube of 15 mm in length and 0.8 mm in diameter. The facility noise was removed from the measured signal using the optimal filtering scheme of Naguib et al. [11]. This required the use of a reference pressure transducer that was positioned at $x^* = -2.15$ and $z^* = 0$ throughout the experiments. The optimal filtering scheme recovers a noise-corrected time series of the fluctuating wall pressure and Trünkle [12] showed that the power spectral density (PSD) of this corrected time series is essentially equal to the PSD obtained with the noise-correction method of Weiss et al. [8].

The analog signals of the piezoresistive pressure transducers were digitized with a 24-bit, National Instruments, NI-PXIe-4492 data acquisition card. The signals were recorded at a sampling rate of 2 kHz for a period of either 300 s or 3600 s. All power spectra were computed using Welch's modified periodogramm method with either 64 or 128 windows, 50% overlap, and a Hamming window [13]. The filter order in the noise-cancellation scheme was set to 4000 [12].

3. Experimental results

3.1. Spanwise variation of pressure fluctuations

Figs. 3 and 4 show the distribution of the static-pressure coefficient $c_p = (p(x^*, z^*) - p_{\text{ref}})/q_{\text{ref}}$ and of the fluctuating-pressure coefficient $c_{p'} = p_{\text{rms}}(x^*, z^*)/q_{\text{ref}}$, respectively. In these notations, the subscript "ref" refers to a quantity measured at the center of the test-section's entrance plane and the subscript "rms" refers to the root mean square of a fluctuating quantity. q_{ref} is the reference dynamic pressure defined as $q_{\text{ref}} = \frac{1}{2}\rho U_{\text{ref}}^2$. Note that all measurements reported in the paper were performed at $U_{\text{ref}} = U_\infty = 25$ m/s and that the Strouhal number is defined as $St = f L_{\text{b}}/U_\infty$ throughout the paper, where $L_{\text{b}} = 0.42$ m is the length of the separation bubble.

The c_p distribution (Fig. 3) shows that the mean detachment occurs at the end of the abrupt pressure rise, while the mean reattachment occurs slightly upstream of the maximum pressure. These characteristics were shown to be consistent with existing data from the literature [8]. Near the reattachment zone, there is a slight difference of c_p between the centerline and the measured sidelines, which is another indication of the three-dimensionality of the near-wall flow, as observed in Fig. 2.

The fluctuating pressure coefficient (Fig. 4) has essentially the same character as the centerline values reported in [8]: the maximum of $c_{p'}$ occurs downstream of the mean reattachment for all spanwise positions and there is a local maximum of $c_{p'}$ at about $x^* = -0.4$ for all spanwise positions except the two positions closest to the walls ($z^* = \pm 2/3$). The global maximum of $c_{p'}$ is mainly caused by the shedding of vortical structures downstream of the separation bubble, whereas the local maximum upstream of the bubble is caused by the low-frequency breathing motion [8].

On the other hand, the large values of $c_{p'}$ at $x^* \simeq 0$ and $z^* = \pm 2/3$ haven't been reported before. Looking at the oil-film visualization of Fig. 2, it appears that this maximum is located very near the two sidewall vortices. As will be shown below,

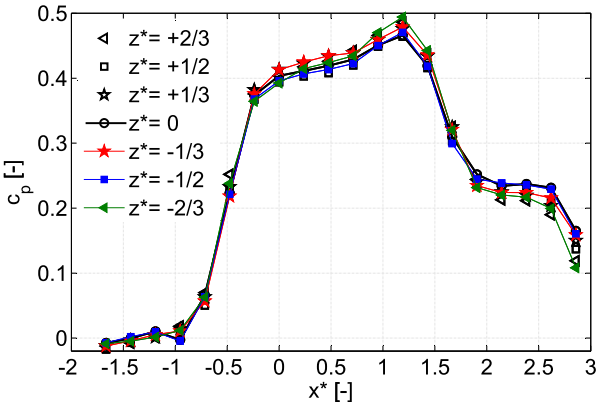

Fig. 3. Pressure coefficient c_p, $U_{\text{ref}} = 25$ m/s.

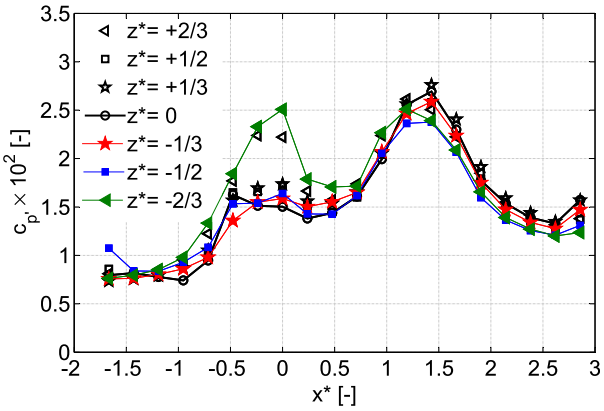

Fig. 4. Fluctuating pressure coefficient $c_{p'}$, $U_{\text{ref}} = 25$ m/s.

the characteristic frequency of the pressure fluctuations at these positions does not correspond to either the shedding or the breathing mode.

3.2. Spectral characteristics

3.2.1. Breathing mode

The low-frequency breathing mode of the separation bubble was reported for the first time by Weiss et al. [8]. It is mainly characterized by a low-frequency wall-pressure fluctuation observed upstream of the mean detachment and downstream of the mean reattachment. On the test-section centerline, the pressure fluctuations at both positions were shown to be highly correlated in the low-frequency range. Fig. 5 shows the streamwise variation of the wall-pressure PSD upstream of the mean detachment point on the tunnel centerline. At $x^* = -0.36$ and $x^* = -0.48$, there is a clear broadband maximum at a normalized center frequency of $St \simeq 0.01$. This low-frequency fluctuation was shown to be linked to a contraction/expansion of the separation bubble dubbed “breathing mode” [8].

The spanwise variation of the PSD is presented in Fig. 6 at a streamwise position of $x^* = -0.48$ (spanwise measurement ports were unfortunately not available at $x^* = -0.36$). The maximum can be clearly identified at a similar frequency for all positions, although the amplitude of this maximum varies. There doesn’t seem to be a specific trend: most values are relatively close to the centerline value, except when $z^* = -1/3$ (lower value) and $z^* = -2/3$ (higher value). The variation of the signal amplitude may possibly be attributed to a small spanwise variation of the detachment line. Indeed, the thermal-tuft measurements of Schwaab and Weiss [10] have shown that the position of the mean detachment slightly varies in spanwise direction, especially between $z^* = -1/3$ and $z^* = -2/3$. Since the measurements reported in Fig. 6 were all made at a fixed streamwise position ($x^* = -0.48$), this means that the separation process might be more or less “advanced” at the $z^* = -1/3$ and $z^* = -2/3$ measurement points. This might explain the difference in amplitude since Fig. 5 shows that the amplitude of the signal is quite dependent of the streamwise position. Note that regardless of this variation in amplitude, the signature of the breathing mode appears to be well established for all spanwise positions.

Fig. 7 shows the magnitude-squared coherence function C_{xy} between two pressure transducers positioned at $x^* = -0.48$ and separated in spanwise direction by a distance Δz^*. C_{xy} is generally fairly small, which tends to imply that the breathing

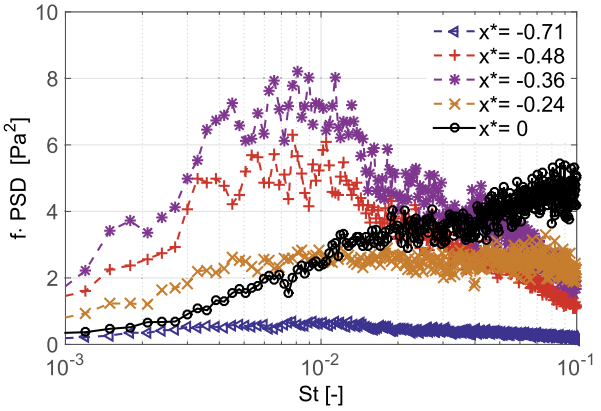

Fig. 5. Streamwise variation of wall-pressure PSD upstream of the separation bubble at $z^* = 0$.

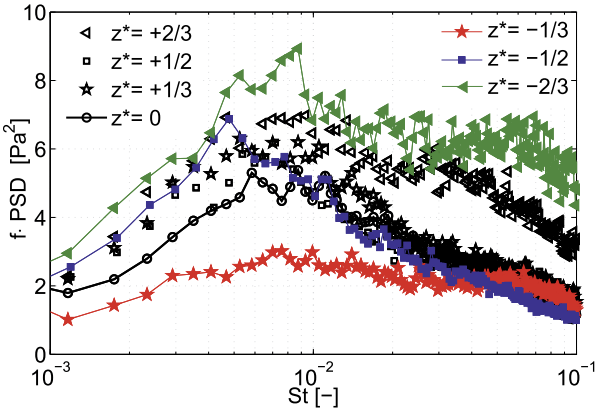

Fig. 6. Spanwise variation of wall-pressure PSD at $x^* = -0.48$.

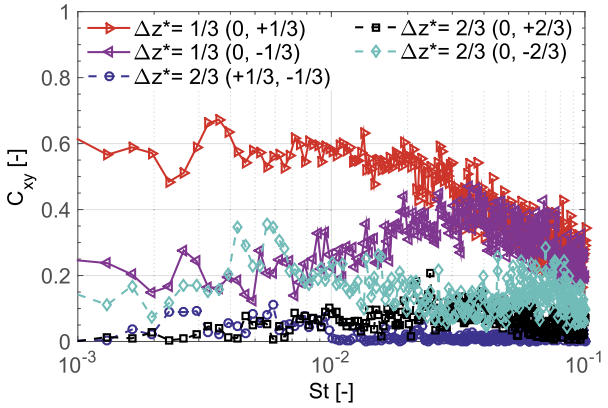

Fig. 7. Coherence function between two spanwise positions at $x^* = -0.48$.

motion is not a spanwise-coherent, two-dimensional contraction and expansion of the bubble, but rather a corrugated motion with limited spanwise length scale. On the other hand, the coherence function between $z^* = 0$ and $z^* = 1/3$ is rather large, suggesting that some unsteadiness is at least coherent between those two spanwise positions. Clearly, measurements with a higher spatial resolution are required in order to better understand this aspect of the flow dynamics.

3.2.2. Shedding mode

The shedding mode in turbulent separation bubbles corresponds to the roll-up and pairing of vortical structures within the separated shear layer and their shedding downstream of the bubble. In fixed-separation flows, the Strouhal number

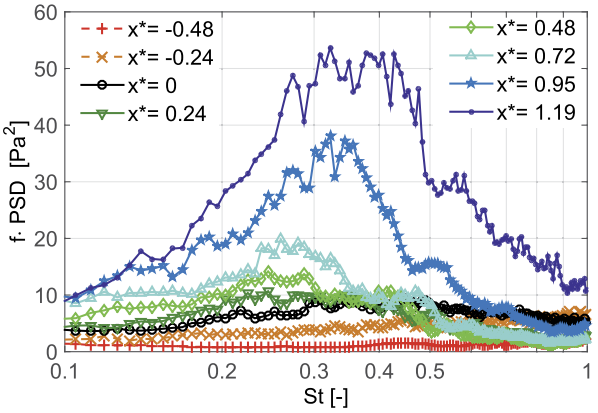

Fig. 8. Streamwise variation of wall-pressure PSD within the separation bubble at $z^* = 0$.

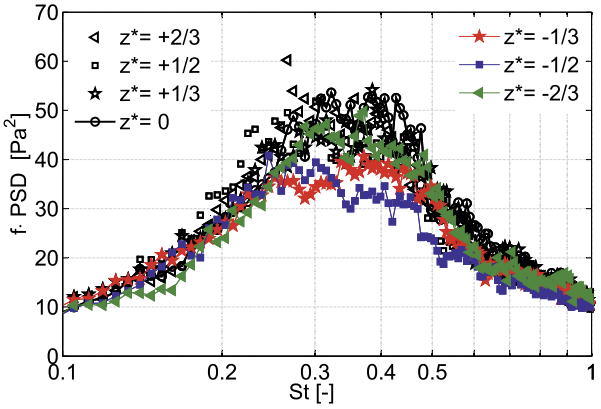

Fig. 9. Spanwise variation of wall-pressure PSD at $x^* = 1.19$.

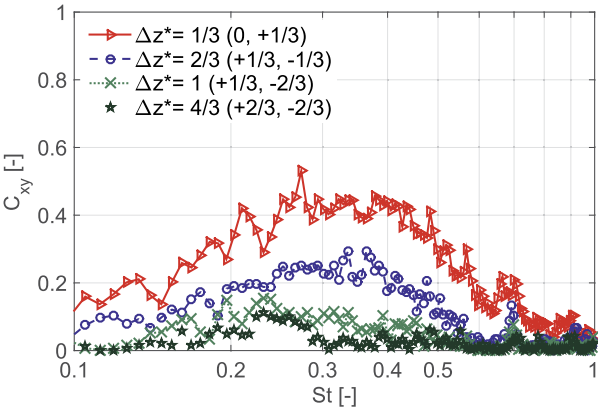

Fig. 10. Coherence function between two spanwise positions at $x^* = 1.19$.

close to reattachment is typically $St = 0.7$ [4]. In pressure-induced separation bubbles, however, the thicker shear layer compared to fixed-separation flows can lead to a lower Strouhal number [8].

In the present flow configuration, Fig. 8 shows that the Strouhal number is close to $St \simeq 0.35$ near reattachment. The increase in energy around this frequency leads to an increase of $c_{p'}$ up to the maximum of $c_{p',\max} \simeq 0.025$ observed in Fig. 4. The spanwise variation of the wall-pressure PSD at $x^* = 1.19$ is presented in Fig. 9. The spectra are almost all superimposed, which shows that the mechanism of vortex formation and shedding is well distributed across the span of the separation bubble.

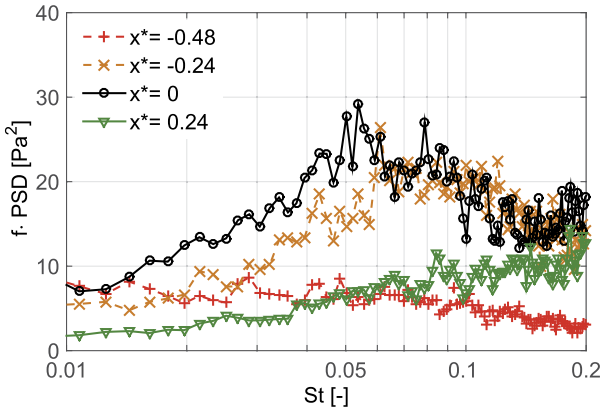

Fig. 11. Streamwise variation of wall-pressure PSD near the sidewall vortex at $z^* = -2/3$.

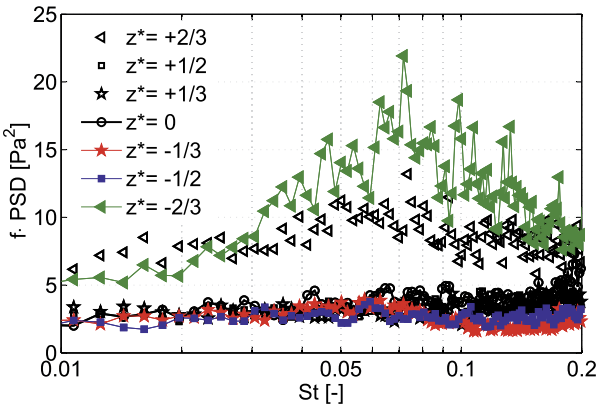

Fig. 12. Spanwise variation of wall-pressure PSD at $x^* = -0.24$.

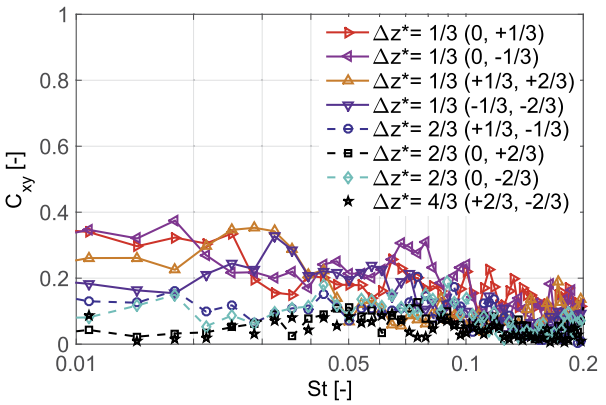

Fig. 13. Coherence function between two spanwise positions at $x^* = 0$.

The same conclusion can be reached by examining Fig. 10, which shows the coherence function C_{xy} in spanwise direction at $x^* = 1.19$. The vortical structures appear to be relatively well correlated up to spanwise distances of $\Delta z^* = 2/3$. This is consistent with the notion of "quasi-2D" vortices forming in the shear layer in a manner similar to what occurs in fixed-separation flows and two-dimensional, turbulent shear layers [14]. For spanwise distances larger than $\Delta z^* = 2/3$, the small-scale turbulent structures of the shear layer tend to destroy the spanwise coherence of the vortices.

3.2.3. Sidewall vortex mode

The streamwise variation of the wall-pressure PSD near the sidewall vortex at $z^* = -2/3$ is shown in Fig. 11. It can be seen that the amplitude near $St \simeq 0.07$ is much larger at $x^* = -0.24$ and $x^* = 0$ than further upstream or downstream.

The same type of phenomenon, albeit with a slightly smaller amplitude, can be observed on the other side of the test section at $z^* = +2/3$, but not between these two spanwise positions. This can be clearly seen in Fig. 12, which shows the spanwise variation of the PSD at $x^* = -0.24$. The increase in energy at $St \simeq 0.07$ is responsible for the peak of $c_{p'}$ at ($x^* \simeq 0$, $z^* = \pm 2/3$) that can be observed in Fig. 4.

Interestingly, the frequency of maximum amplitude is different than that corresponding to the breathing or the shedding mode. Furthermore, the positions of maximum amplitude are located very close to the slow-moving vortices that occur near the sidewalls and that are visible in the oil-film image of Fig. 2. This suggests that the increase in pressure fluctuations may be caused by the vortices themselves. Trünkle [12] also measured the fluctuating wall pressure in an asymmetric flow that was created by slightly skewing the geometry of the test section. The oil-flow picture that was obtained was highly asymmetric, although the spectral characteristics of the pressure fluctuations were relatively insensitive to the near-wall flow skewing. On the other hand, the positions where the sidewall fluctuating mode was measured had changed and corresponded to the new positions of the sidewall vortices. This is further evidence that the $St \simeq 0.07$ mode observed in Figs. 11 and 12 is indeed a consequence of the slow-moving sidewall vortices.

Finally, the coherence function C_{xy} at $x^* = 0$ between several spanwise positions is presented in Fig. 13. The value of C_{xy} near $St \simeq 0.07$ is quite low for all pairs of positions. This is consistent with the idea of highly localized pressure fluctuations and this corroborates our argument that the $St \simeq 0.07$ mode is indeed linked to the sidewall vortices.

4. Conclusion

Fluctuating wall-pressure measurements were performed on the test surface above a pressure-induced, turbulent separation bubble. The results confirm the presence of a low-frequency breathing mode, caused by the contraction and expansion of the bubble, and a medium-frequency shedding mode, caused by the convective roll-up of spanwise vortices in the shear layer bordering the recirculating region. As shown in [8], the Strouhal number of both modes ($St_{\text{breathing}} \simeq 0.01$ and $St_{\text{shedding}} \simeq 0.35$) is much lower than the normalized frequency of turbulent structures in the flow. In addition, a third fluctuating mode with a Strouhal number $St_{\text{sidewall}} \simeq 0.07$ was observed near the sidewalls of the test section close to the mean detachment line. This latter mode is interpreted as a consequence of the presence of slowly rotating vortices close to the test-section sidewalls.

The signatures of both the breathing and the shedding modes appear clearly throughout the span of the test section, which shows that both modes are relatively insensitive to the three-dimensional aspect of the near-wall streamlines. Mohammed-Taifour and Weiss [15] have shown that the off-wall geometry of the separation bubble varies less in spanwise direction than the near-wall streamlines. This tends to show that the breathing and shedding modes are more related to the global geometry of the bubble than to the spanwise-sensitive, near-wall flow. Coherence measurements clearly showed that the vortices causing the shedding mode are fairly correlated in the spanwise direction. On the other hand, no clear conclusion could be obtained regarding the spanwise coherence of the breathing mode.

Acknowledgements

Part of this work was supported by the Natural Sciences and Engineering Research Council of Canada and the Fonds de recherche du Québec – Nature et technologies. The first author was supported by a grant from the Hermann–Reissner Foundation during his stay at the TFT lab.

References

[1] D.M. Driver, H.L. Seegmiller, J.G. Marvin, Time-dependent behavior of a reattaching shear layer, AIAA J. 25 (7) (1987) 914–919.
[2] M. Kiya, K. Sasaki, Structure of a turbulent separation bubble, J. Fluid Mech. 137 (1983) 83–113.
[3] N. Cherry, R. Hillier, M. Latour, Unsteady measurements in a separated and reattaching flow, J. Fluid Mech. 144 (1984) 13–46.
[4] L.M. Hudy, A.M. Naguib, W.M. Humphreys Jr., Wall-pressure-array measurements beneath a separating/reattaching flow region, Phys. Fluids 15 (3) (2003) 706–717.
[5] N.T. Clemens, V. Narayanaswamy, Low-frequency unsteadiness of shock wave/turbulent boundary layer interactions, Annu. Rev. Fluid Mech. 46 (2014) 469–492.
[6] J.-P. Dussauge, P. Dupont, J.-F. Debiève, Unsteadiness in shock wave boundary layer interactions with separation, Aerosp. Sci. Technol. 10 (2) (2006) 85–91.
[7] P. Dupont, C. Haddad, J. Debiève, Space and time organization in a shock-induced separated boundary layer, J. Fluid Mech. 559 (2006) 255–277.
[8] J. Weiss, A. Mohammed-Taifour, Q. Schwaab, Unsteady behavior of a pressure-induced turbulent separation bubble, AIAA J. 53 (9) (2015) 2634–2645.
[9] A. Mohammed-Taifour, Q. Schwaab, J. Pioton, J. Weiss, A new wind tunnel for the study of pressure-induced separating and reattaching flows, Aeronaut. J. 119 (1211) (2015) 91–108.
[10] Q. Schwaab, J. Weiss, Evaluation of a thermal-tuft probe for turbulent separating and reattaching flows, J. Fluids Eng. 137 (2015) 011401, 7 p.
[11] A.M. Naguib, S.P. Gravante, C.E. Wark, Extraction of turbulent wall-pressure time-series using an optimal filtering scheme, Exp. Fluids 22 (1996) 14–22.
[12] J. Trünkle, Measurements of wall static-pressure fluctuations in a turbulent separation bubble, Master's thesis, University of Stuttgart, 2014.
[13] J.S. Bendat, A.G. Piersol, Random Data: Analysis and Measurement Procedures, 3 ed., John Wiley & Sons, 2010.
[14] T.R. Troutt, B. Scheelke, T.R. Norman, Organized structures in a reattaching separated flow field, J. Fluid Mech. 143 (1984) 413–427.
[15] A. Mohammed-Taifour, J. Weiss, Écoulement moyen dans une bulle de décollement turbulente, in: Proceedings of The 2014 International Congress of Canadian Society for Mechanical Engineering, 2014.